Atmos. Chem. Phys. Discuss., 11, 26415–26440, 2011
www.atmos-chem-phys-discuss.net/11/26415/2011/
doi:10.5194/acpd-11-26415-2011

Atmospheric Chemistry and Physics Discussions

Teleconnection between Australian winter temperature and Indian summer monsoon rainfall

S.-Y. Lee[1] and T.-Y. Koh[1,2]

[1]School of Physical and Mathematical Sciences, Nanyang Technological University, Singapore
[2]Earth Observatory of Singapore, Nanyang Technological University, Singapore

Received: 1 July 2011 – Accepted: 14 September 2011 – Published: 22 September 2011

Correspondence to: T.-Y. Koh (kohty@ntu.edu.sg)

Published by Copernicus Publications on behalf of the European Geosciences Union.

Abstract

The large-scale circulation over the Indian Ocean during the boreal summer raises the question of whether atmospheric conditions in Australia could influence conditions over the Indian subcontinent, despite the long passage of air over the Indian Ocean. Using a combination of reanalysis, satellite and in situ data, we argue that unusually low temperature over inland Australia during austral winter can enhance evaporation rate over the eastern tropical Indian Ocean, and hence enhance rainfall over western India after 10–18 days. Since extreme winter temperature in Australia is often associated with cold-air outbreaks, the above mechanism can be an example of how southern hemispheric mid-latitude weather can influence northern hemispheric monsoon rainfall.

1 Introduction

The Indian summer monsoon displays huge variability with interannual and intraseasonal components, though there are varied opinions on how much of the interannual monsoon variability is the mean expression of intraseasonal variability, and how much of the intraseasonal variability is actually interannual variability. Comparisons of empirical orthogonal functions have yielded different results. Some findings favour intraseasonal dominance (e.g. Goswami and Mohan, 2001; Lawrence and Webster, 2001), others favour interannual dominance (e.g. Singh et al., 1992; Annamalai et al., 1999; Sperber et al., 2000; Krishnamurthy and Shukla, 2000). Although opinions vary on the extent of their influence, it is generally agreed upon that interannual phenomena such as the El Nino-Southern Oscillation (ENSO) (Rasmusson and Carpenter, 1983) and Indian Ocean Dipole (IOD) (Saji et al., 1999) have significant influence on Indian monsoon rainfall. ENSO and IOD are measured by the various Nino indices (see Hanley et al., 2003, for a comparison) and the Dipole Mode Index (DMI) respectively.

The above-mentioned literature focused on tropical climatic patterns. Other studies consider northern hemispheric influences on the monsoon, such as the Eurasian snow cover (Hahn and Shukla, 1976; Kripalani and Kulkarni, 1999; Liu and Yanai, 2002). Less has been said about interaction between the Southern Hemisphere and Indian monsoon. There are works that investigated the reverse influence of monsoon variability in northern Australia, e.g. Matsumoto (1992) and Krishnamurti et al. (1995). The Indian summer monsoon is correlated with the next Australian summer monsoon in both onset date (Joseph et al., 1991) and strength (Gregory, 1991). Meehl (1987, 1997) explains this relationship as due to the intense convection in a strong Indian monsoon migrating southeast to Australia as the year progresses, producing a strong Australian monsoon. Incidentally, there is no analogous effect of Australian monsoon on the next Indian summer monsoon (Hung et al., 2004).

As for the influence of the Southern Hemisphere on Indian monsoon variability, it is known that the sea surface temperature (SST) near Australia influences Indian monsoon rainfall. The example of SST influence reported in Nicholls (1995) appears to be part of the ENSO/IOD pattern, but Clark et al. (2000) showed that after excluding ENSO influences, the preceding boreal spring SST north of Australia does have a residual impact on Indian monsoon rainfall.

So, not detracting from the important influence of tropical climatic variations like ENSO and IOD, and the influence of austral tropical SST on Indian summer monsoon, this paper aims to show that there may exist a dynamically plausible way for Australian weather to influence Indian summer monsoon. If so, further investigation into this possibility would be warranted.

2 Motivation

The large-scale circulation over the Indian Ocean during the boreal summer suggests the question of whether atmospheric conditions in Australia can influence those over the Indian subcontinent, despite the long passage of air over the Indian Ocean. The motion of water vapour in the region is recapitulated in Fig. 1, which shows in shading the net climatological source of water vapour in an air column. This is calculated from

ACPD
11, 26415–26440, 2011

the convergence of vertically integrated water vapour flux (shown as arrows) and the time-tendency of water vapour (not shown, but small), using data from the Japanese 25-yr Reanalysis. The data has been pentad-averaged and lanczos-filtered to remove Gibbs ringing. This results in the weakening of quantitative magnitudes compared to existing literature (e.g. Peixoto and Oort, 1992) but retains the qualitative patterns of water vapour sources and sinks.

Following the clockwise circulation over the Indian Ocean, air picks up moisture from west of Australia and the Indian Ocean (red shading). Moisture precipitates out in the eastern Arabian sea, west coast of India, northeast India and Bay of Bengal (dark green and blue). Southeast India, in the rain shadow of the Western Ghats, appears as a weak sink or even source of moisture (light green and yellow).

Since a non-negligible source of moisture in this system lies just off the coast of Australia, the temperature and humidity of air parcels entering the large scale circulation from Australia would affect the evaporative flux in this region. This suggests the question of whether meteorological conditions over Australia can result in variability in this regional evaporative flux and subsequently affect precipitation in India.

With this in mind, we hypothesize the existence of a different type of teleconnection between Australia and India that does not arise through simultaneous driving by an external variability (e.g. ENSO or IOD): if the originating conditions are extremely cold and hence dry over interior Australia during austral winter, the rainfall in the same-season Indian monsoon is enhanced via increase in evaporation over eastern tropical Indian Ocean (henceforth "Australia-Indian teleconnection"). If there is such an influence, it should be present only in regions of India where air parcels originating from Australia pass over the Indian Ocean and directly offload their moisture content onto India. Therefore, we expect a teleconnection in west India, but not in southeast India (because the air flow has already offloaded their moisture on west India). It is more uncertain if there will be a teleconnection in northeast India. Reanalysis, satellite and in-situ data will be examined for consistency with this hypothesis.

Discussion Paper | Discussion Paper | Discussion Paper | Discussion Paper |

ACPD

11, 26415–26440, 2011

Australia-India teleconnection

S.-Y. Lee and T.-Y. Koh

2.1 Organisation

This paper is organized as follows: Sect. 3 provides the details of the data and methods adopted in this research, leaving Sect. 4 to focus on the main results and their interpretation. The key conclusions are stated in Sect. 5.

3 Data and methodology

3.1 Back-trajectory calculations

To demonstrate the possible pathway by which Australia may be able to influence Indian rainfall, back-trajectories are calculated for up to 30 days using 6-hourly winds from the NCEP/NCAR Reanalysis 1 dataset (Kalnay et al., 1996, henceforth "NNRP"). Air parcels are placed over land regions of the Indian sub-continent 0.25° apart on pressure levels 1000 mb, 925 mb, and 850 mb. Trial calculations show few air parcels from higher levels over India come from Australia at near-surface levels. Calculations are started at the end of austral winter months of June, July and August (JJA) for years 1980–2009.

The diagonal line from (120° E, 30° S) to (135° E, 15° S), shown in Fig. 2a as a diagonal magenta line, is used as the end point for the calculation of trajectory times. This is where many back-trajectories pass over before meeting the Macdonnell Ranges. Back-trajectories that reach Australia are classified as coming from the domains of "Entire India" (68–93° E, 6–31° N), "West India" (68–78° E, 8–30° N) and "East India" (78–93° E, 6–28° N), which are the land regions of the red boxes in Fig. 2b. Some trajectories originating from the centre of India can belong to both east and west domains because they pass over both before leaving India.

ACPD
11, 26415–26440, 2011

3.2 Satellite rainfall and reanalysis temperature

If the hypothesis in Sect. 2 is correct, there should be a lagged anti-correlation between the Australian temperature and Indian rainfall. Furthermore, the lag period for maximum anti-correlation should be consistent with the trajectory times obtained from Sect. 3.1.

To estimate Australian winter temperature, the daily mean temperature at 0.995 sigma-level from NNRP is averaged over a polygonal region within 115–105° E, 35–15° S, shown in Fig. 2a as a magenta polygon. This region is where most back-trajectories reaching Australia pass through. The reason for the polygonal shape is to exclude ocean and coastal regions. Highland regions are included but the exclusion of highland regions is also attempted and does not lead to qualitative differences. The temperature time series is passed through a 8-days-to-2-months Lanczos band-pass filter to exclude synoptic fluctuations and seasonal signature, including harmonics of the seasonal signature (see Appendix A for the reason behind the choice of 8 days for the higher cut-off frequency). This extracts the intraseasonal signature.

Rainfall in India is provided by the Tropical Rain Measuring Mission (TRMM) 3B42 dataset which is calibrated to rain gauges and geostationary observations for years 1998–2008. The coverage is 8x-daily at 0.25° × 0.25° resolution. TRMM data is available every 3 h and but a daily time series is computed for correlation with the daily mean Australian temperature. Each day's rainfall value is the average of all available TRMM data points in a given domain spanning the 8 time slices of that day. A 8-days-to-2-months Lanczos band-pass filter is applied here as well.

Pearson's correlation between the temperature and rainfall time series is calculated for various time lags. Thresholds are imposed at different temperature percentiles to eliminate warmer temperatures and the corresponding lagged rainfall data, since only cold temperature is believed to be related to Indian rainfall.

ACPD
11, 26415–26440, 2011

3.3 Regression of in-situ data

While analysed temperature and TRMM rainfall data provide good horizontal coverage, in-situ station and rain gauge measurements provide longer historical records and hence supply supplementary evidence for the Australia-India teleconnection.

At first sight, the mean of Australian station temperature intuitively corresponds to the mean of gridded reanalysis temperature. But it actually does not because of the highly uneven density of stations in Australia. Stations are concentrated in southeast Australia and sparsely distributed over the northwest and interior regions. The Australian Bureau of Meteorology (BOM) maintains a long yearly record of the number of very cold days in a year averaged over stations ("VCD"), where a very cold day is one when the maximum day temperature is below 10 °C. When many stations across Australia (especially those in the southeast) record a very cold day, the entire air mass over Australia, including the less and unobserved regions, is likely to be anomalously cold with respect to the local winter climatology. Thus VCD can be used as an in-situ proxy for extreme coldness over the whole of Australia. Appendix A further supports the use of this proxy by comparing VCD and mean Australian temperatures by percentile, from NNRP reanalysis data.

The daily accumulated in-situ rainfall comes from individual rain gauges in the National Oceanic and Atmospheric Administration (NOAA) archive. The period of 1977–2008 is selected to obtain the largest number of gauges for a continuous period longer than 30 yr, and with at least 26 out of the 32 summer seasons each, or 80 % of the 32 seasons, having at least 30 days of data. Such selection criteria for the gauges ensures that the seasonal mean rainfall obtained is representative. The rain gauge data is not time-filtered to avoid the need to estimate missing data which may produce spurious oscillations of the timescales in question and therefore degrade the value of in-situ measurements.

The mean rainfall from 18 June to 17 September (i.e. JJA lagged by 17 days for the approximate travel time of air parcels) is calculated every year and correlated against

ACPD
11, 26415–26440, 2011
Australia-India teleconnection
S.-Y. Lee and T.-Y. Koh

VCD. Although the monsoon season extends beyond this time period, the length of the temperate winter season limits the time period to be considered.

3.4 Comparison with climatic indices

It is possible that interannual variations in VCD are related to interannual climatic patterns like ENSO and IOD. This means that any correlation between Indian rainfall and VCD could be due to the dependence on ENSO and IOD phases and should be investigated.

The DMI used to denote the phase of IOD is obtained from Japan Agency for Marine-Earth Science and Technology (JAMSTEC); Nino3 and Nino3.4 indices for denoting the phase of ENSO are from NOAA. VCD is correlated with the mean DMI of August, September and October (ASO) and with the mean Nino3.4 and Nino4 indices of December, January and February (DJF). These are separately the months when IOD and ENSO SST anomalies are usually the largest, and ensures that IOD or ENSO events can be captured even if the respective indices at JJA do not indicate developing events yet. Since ENSO spans more than one year, both VCD from the same (ENSO-developing) and from the following (ENSO-mature) year to the December month in the Nino indices are used.

3.5 Sea surface evaporation data

In the course of exploring the mechanism underlying the Australia-India teleconnection, evaporation from Indian Ocean and associated factors are investigated. Monthly mean evaporation rate, specific humidity at 2m and SST over the ocean at $1^{\circ} \times 1^{\circ}$ resolution are taken from the Objectively Analyzed Air-Sea Fluxes dataset (OAFlux) of Woods Hole Oceanographic Institution (Yu et al., 2007). Since only wind magnitudes but not wind vectorial components are available in OAFlux, NNRP 10m-wind is used instead. Although this wind field is not the same as that used to calculate the evaporation rate in OAFlux, it is one of the inputs used to estimate the OAFlux wind and so is expected to be similar. JJA mean anomalies are computed from 1958–2008 JJA climatology.

3.6 A note on reanalysis data

The results presented here that make use of the NNRP dataset have been checked using the Japanese 25-yr Reanalysis (Onogi et al., 2007) obtained from Meteorological Research Institute (MRI), Japan Meteorological Agency (JMA). The different choice of reanalysis dataset does not alter the results much because low-level wind and surface air temperature in reanalysis datasets are strongly constrained by observations. In the case of Fig. 1, the Japanese Reanalysis was used due to its higher horizontal resolution.

4 Results and discussion

4.1 Back-trajectories from India to Australia

Figure 2 shows the number density of air parcel back-trajectories between Australia and India, which are counts of how many trajectories have passed over each $0.25^{\circ} \times 0.25^{\circ}$ grid box. There are three clusters of back-trajectories that follow two branches of the Indian monsoon: two clusters pass over the Arabian Sea separately reaching west and northwest India; the third cluster passes over the Bay of Bengal reaching northeast India. The extremely high number density over northeast India is due to the high terrain of Myanmar and the Himalayas obstructing and funneling trajectories northwest-wards over a narrow region. About three percent of all the back-trajectories initiated over India originate from Australia. However the percentage varies from region to region. This number can reach up to about ten percent in certain regions of West India, while extremely few back-trajectories initiated over the southeast and east regions of India originate from Australia.

Figure 3a–c show the differences in trajectory times for back-trajectories from the Entire India, East India and West India domains. When back-trajectories from the Entire India domain are considered, the trajectory times show a wide spread from

13–27 days (Fig. 3a). This is because the back-trajectories originating from the East India domain and the West India domain have different spreads of trajectory times. 13–18 day trajectories dominate in the West India domain, having mostly come through Arabian Sea (Fig. 2a and 2b). Most of the back-trajectories that originate in Australia were initiated over the West India domain.

4.2 Satellite rainfall and reanalysis temperature

Figure 3d–f show the lag correlation between NNRP Australian temperature and TRMM rainfall for the three domains. In Fig. 3d for the Entire India domain, a broad W-shaped anti-correlation trough can be seen for lags of more than 10 days. The left branch of the trough seems to correspond to the 13–18-day trajectories and the right branch to the 20–27-day trajectories (shaded bars). Both anti-correlation troughs while significant, are quite weak, with correlation coefficients between −0.10 and −0.30. (The positive ridge at 5 days and the negative trough at −15 days are ignored as they arise from the autocorrelation in rainfall on intraseasonal timescale.) However, when only the West India domain is considered and warm temperatures are excluded leaving only the coldest 30th percentile, the strength of anti-correlation in the left branch increases to between −0.2 and −0.4.

We next considered when the rainfall domain is restricted to East India (Fig. 3e) or West India (Fig. 3f) only. In Fig. 3e, both troughs have almost disappeared together with the reduced relative population of trajectories (Fig. 3b). Although there remains some 20–27-day trajectories, the right trough is no longer present, indicating that there is no significant relationship between rainfall in the East India domain and Australian winter temperature. In Fig. 3f, both troughs are retained. For the left trough, the anti-correlation between the cold temperatures and rainfall in the West India domain becomes more apparent. The right trough is weakened and much of it disappears following the lessened population of the 20–27 day trajectories, especially those of shorter travel times. It is clear that the rainfall in these two domains should be considered separately. We focus henceforth on West India, where a greater fraction of air parcels

ACPD
11, 26415–26440, 2011

originate from Australia, and take special note of the shorter travel times of 13–18 days because the plausible influence from Australia is less likely to be complicated by other factors during the parcels' journey and stronger anti-correlation exists at such time lags in Fig. 3f.

4.3 In-situ observations

The location of the Indian rain gauges used for the correlation with VCD is plotted in Fig. 2b. Magenta squares show gauges where the there is significant correlation between VCD and seasonal mean rainfall at 95 % confidence level. The correlation values for these gauges are shown in Table 1.

6 out of 19 gauges in the West India domain individually show significant Australia-India teleconnection at 95 % confidence level, and they lie in regions where air parcels coming from Australia via the Arabian Sea are orographically lifted (see magenta squares in West India box in Fig. 2b). This fraction is higher than 3 out of 19, the threshold below which the field correlation (Wilks, 1995, also Appendix B for easy reference) of West Indian rainfall with VCD is not significant at 95 % confidence level. Moreover, why the other gauges in West India do not show significant Australia-India teleconnection might be understood: they lie either in the rain shadow of high terrain or over arid or semi-arid plains where orographic lifting does not occur, so that any enhanced moisture content from the teleconnection does not manifest as rain (Sect. 2). Mumbai (72.9° E, 18.9° N) and Cochin (76.6° E, 10.0° N) are the only exceptions where perhaps other influences dominate.

There is no significant field correlation between rainfall in the East India domain and VCD at 95 % confidence level.

4.4 Climatic indices

ENSO and IOD are known to have impacts on Australia (Meyers et al., 2007) Therefore it is possible that the Australia-India teleconnection is part of these two tropical climatic

ACPD
11, 26415–26440, 2011

patterns. Correlation of VCD separately with Nino3.4 (Fig. 4a), Nino4 (not shown) and DMI (Fig. 4b) does not yield significant results. The lack of relationship between VCD and ENSO or IOD shows that the teleconnection is not due to the coordinated impact of ENSO or IOD on Australia temperature and rainfall in the West Indian domain. This may be understood as ENSO and IOD are tropical patterns while VCD measures temperature over all of Australia inclusive of subtropical and mid-latitude regions.

4.5 Possible mechanism

The results of the previous sections are consistent with the proposed Australia-India teleconnection for which we propose the following mechanism: the advection of cold dry Australian air from southeast to northwest over the Indian Ocean where the enhanced evaporation rate ultimately feeds the enhanced rainfall rate downstream in West India.

As Australia lies mostly in the subtropics and is subjected to oceanic influences, winters in Australia are generally mild. But extreme lows in Australia winter temperature are commonly associated with subseasonal cold spells or "cold-air outbreaks", which are due to mid-latitude baroclinic wave activity. This is especially so since the stations from which VCD is computed are clustered in southeast Australia. Cold-air outbreaks from 1972 to 1991 have been tabulated by Perrin and Simmonds (1995) and Simmonds and Richter (2000) using percentile temperature thresholds as criteria. They occurred in all five coldest years (i.e. the coldest quartile) ranked by VCD in this period: 1978, 1983, 1986, 1990, 1981 (in decreasing coldness). This suggests that cold-air outbreaks in Australia is a likely cause of extreme low temperatures. How such low Australian temperature promote rainfall in West India is explored next.

Very low winter temperature implies that air over Australia has very low saturation vapour pressure, and hence very low specific humidity. Recalling Fig. 1, this air warms up as it moves across Australia and over tropical Indian Ocean. We show below that evaporative fluxes calculated from observations and reanalyzed dynamical variables are consistent with the picture of remote influence of cold-air outbreaks on Indian rainfall.

ACPD
11, 26415–26440, 2011
Australia-India teleconnection
S.-Y. Lee and T.-Y. Koh

Figure 5a shows the composite pattern of enhanced evaporation in the five extreme years mentioned above, with three possible a priori causes: drier surface air, stronger surface wind, and/or warmer SST. The extent of the significant positive evaporation rate anomalies just west of Australia corresponds to that of the significant negative specific humidity anomalies at 2 m height (Fig. 5b). The significant 10 m-wind anomalies (magenta arrows in Fig. 5a) lie offshore of East Africa but does not overlap with any sigificant anomalies of evaporation rate. The SST anomalies (Fig. 5c) overlapping with the region of significant enhanced evaporation are negative and so tend to retard evaporation rate, suggesting instead that cold SST anomalies may be the effect of enhanced evaporation rather than the cause. Thus, drier surface air and not surface wind perturbations or warm SST is the more likely reason for the enhanced evaporation rate. SST anomalies north of Australia are positive but while such SST anomalies have been noted to correlate with Indian monsoon rainfall by Nicholls (1995), they were employed as proxies for ENSO. In this case and consistent with the last section, neither the SST nor the surface wind anomalies closely resemble ENSO or IOD anomalies which affect evaporation, and the years in the composite are variously neutral, negative or positive in ENSO and IOD phases (cf. Meyers et al., 2007). The influence of ENSO, if any, would be indirect – Nicholls (1989) pointed out that the anomalies in the SST north of Australia can also be a consequence of large-scale winter cloud bands that form when tropical air is pushed above intrusions of cold air from the mid-latitudes (Tapp and Barrell, 1984), and ENSO phases alter the frequency of such cloud band formations (Kuhnel, 1988). Indeed, the SST anomalies obtained here have a pattern that resembles that associated with the cloud bands, rather than ENSO.

We note that the transport of mid-latitude air to tropical regions leading to enhanced tropical rainfall is not unheard of. In the Northern Hemisphere, air mass over the Asian continent has been observed to be transported to northwest of Borneo (Chang et al., 1979) during boreal winter. These cold surges are a combination of cold-air outbreaks and the Asian winter monsoon flow, and result in increased low-level convergence which then enhances convection in southern South China Sea. The transport

ACPD
11, 26415–26440, 2011

Australia-India teleconnection

S.-Y. Lee and T.-Y. Koh

of mid-latitude air from Australia to eastern tropical Indian Ocean is the Southern Hemisphere's analogue of the Asian cold surge. The strength of the low-level monsoon circulation brings the mid-latitude influence further, resulting in a cross-equatorial impact on West India.

Figure 5d shows the distribution of the rain gauges where the seasonal mean daily rainfall is anomalously high for the same five extreme years mentioned above. The distribution of rain gauges showing the Australia-India teleconnection in Fig. 2b is also consistent with this understanding.

Although the Australia-India teleconnection is demonstrated from in-situ observations on the interannual or longer timescale, this is due to VCD being a yearly statistic. Interannual patterns and long-term trends affect Australian temperature and the teleconnection mechanism does not differentiate between the reasons for unusually cold temperature. Nevertheless, even when the seasonal signature is removed as carried out in Sect. 4.2, sub-seasonal periods of low winter temperature in Australia can still promote sub-seasonal periods of rainfall in the West India domain.

5 Conclusions

A mechanism for a teleconnection between Australian temperature and monsoon rainfall in west India is proposed: dry air advecting northwestward out of a cold Australia enhances evaporation rate over eastern tropical Indian Ocean, which is balanced by enhanced rainfall rate when the air parcels experience orographic lifting in West India.

A fraction of air over India, especially West India, does originate from Australia, as demonstrated from the back-trajectories (Fig. 2a, b). This air passes over the ocean just west of Australia which constitutes a non-negligible source of water vapour for the Indian summer monsoon (Fig. 1). Figure 5a–c show higher evaporation and drier air over the ocean just west of Australia during outbreak years, which is consistent with the hypothesis that colder air travelling westwards from Australia results in drier air over the ocean just west of Australia and enhances evaporation. In addition, the

SST west of Australia is anomalously cold during the outbreak years, excluding the other possibility of warmer SST enhancing evaporation. Unfortunately, there is a lack of direct horizontal water vapour flux observations to show enhanced transport from Australia to India in cold-air outbreak years, and reanalysis datasets are too much subjected to uncertainties in model parameterization for tropical convective rainfall to show reliably or significantly the flux anomalies for composites of a few years.

Nonetheless, a statistically significant field correlation (Wilks, 1995, also Appendix B for easy reference) was found to exist between VCD and gauge rainfall over a long time base (32 yr) (Fig. 2b). Gauge rainfall is also anomalously high in the outbreak years (Fig. 5d). The correlations in Table 1 are comparable to those of operational predictors for total seasonal rainfall in India. E.g. Indian Ocean SST anomaly, North Atlantic SST anomaly and European land surface air temperature anomaly have correlations of 0.52, −0.45 and 0.42 respectively (Rajeevan et al., 2007) with Indian ranfall. However, the caveat is that the relation is only useful for certain regions in West India. Examination of VCD and individual gauges reveal that both contain a downward trend, but this is consistent with the hypothesized mechanism that a warmer Australian climate would reduce the mean evaporation into air parcels over the ocean just west of Australia.

Statistically significant lagged correlation between NCEP temperature and TRMM rainfall over 11 yr demonstrate the correct time delay between cold temperature anomaly and rainfall enhancement within a season, as expected from back-trajectory travel times (Fig. 3a–f).

The proposed influence is not directly linked to ENSO and IOD (Fig. 4), but does not detract from the dominant influence of ENSO and IOD on Indian rainfall – while these influences are well-known and most important, some of the rainfall variability on subseasonal, interannual or longer timescales may be influenced by conditions as far away as mid-latitude Australia.

ACPD
11, 26415–26440, 2011

S.-Y. Lee and T.-Y. Koh

Appendix A

VCD as a proxy

It is reasoned dynamically in Sect. 3.3 that VCD is a proxy for extreme cold over Australia. Here we show that VCD is indeed related to the percentile mean temperatures in Australia calculated in Sect. 3.2.

Figure A1 shows the correlation coefficient between VCD and the percentile mean temperatures in Australia after applying an *n*-day-to-2-months bandpass filter to the temperature, using different *n*. Shaded regions are where the correlation coefficient is significantly non-zero at 90 % confidence level. There is significant anti-correlation between VCD and the mean percentile temperature, about −0.5 to −0.6, over a wide range of *n* and temperature percentiles. The lack of significance for lower temperature percentiles with increasing *n* is likely to be due to the reduced amplitude of temperature fluctuations after filtering. However, with less filtering the correlation suffers, as can be seen from the region of $n < 7$ and sub-40 percentiles in Fig. A1.

It can be seen that VCD is indeed representative of low temperatures in Australia. Furthermore, while low temperatures as counted by VCD are affected by interannual fluctuations in the amplitude of the seasonal cycle, even with seasonal signals removed the sub-seasonal signals have a significant effect on temperatures.

Appendix B

Field significance

Significance testing repeated at a large number of local points (in this case, rain gauges) will inevitably yield false positives by chance. Field significance tests whether the positives obtained in the entire set of points arise from chance.

ACPD
11, 26415–26440, 2011
Australia-India teleconnection
S.-Y. Lee and T.-Y. Koh

Following Livezey and Chen (1983) and Wilks (1995), we wish to know what is the minimum number of gauges needed out of the 19 gauges in West India, to be certain the positive results did not come about by chance, at $\alpha = 0.05$ (i.e. 95 % confidence level).

Probability(0 of 19) $= {}^{19}C_0(0.95)^{19} = 0.34$

Probability(1 of 19) $= {}^{19}C_1(0.95)^{18}(0.05) = 0.38$

Probability(2 of 19) = 0.18

Probability(3 of 19) = 0.05

Probability(more than 3 of 19) = 0.05

Therefore, it is required that more than 3 gauges out of 19 gauges in west India test positive to demonstrate a significant relationship at confidence level 95 %.

Acknowledgements. We would like to thank: BOM, JMA/MRI, JAMSTEC, NASA/JAXA, NCEP/NCAR, NOAA and WHOI for use of their datasets; I. Simmonds and K. Keay for the trajectory code; and C. K. Teo for extracting the TRMM data; the anonymous reviewers for their comments.

References

Annamalai, H., Slingo, J., Sperber, K., and Hodges, K.: The mean evolution and variability of the Asian summer monsoon: Comparison of ECMWF and NCEP-NCAR reanalyses, Mon. Weather Rev., 127, 1157–1186, 1999. 26416

Chang, C., Erickson, J., and Lau, K.: Northeasterly cold surges and near-equatorial disturbances over the winter MONEX area during December 1974 .1. Synoptic aspects, Mon. Weather Rev., 107, 812–829, 1979. 26427

Clark, C., Cole, J., and Webster, P.: Indian Ocean SST and Indian summer rainfall: Predictive relationships and their decadal variability, J. Climate, 13, 2503–2519, 2000. 26417

Goswami, B. and Mohan, R.: Intraseasonal oscillations and interannual variability of the Indian summer monsoon, J. Climate, 14, 1180–1198, 2001. 26416

Gregory, S.: Interrelationships between Indian and Northern Australian summer monsoon rainfall values, Int. J. Climatol., 11, 55–62, 1991. 26417

Hahn, D. and Shukla, J.: Apparent relationship between Eurasian snow cover and Indian monsoon rainfall, J. Atmos. Sci., 33, 2461–2462, 1976. 26417

Hanley, D., Bourassa, M., O'Brien, J., Smith, S., and Spade, E.: A quantitative evaluation of ENSO indices, J. Climate, 16, 1249–1258, 2003. 26416
Hung, C., Liu, X., and Yanai, M.: Symmetry and Asymmetry of the Asian and Australian Summer Monsoons, J. Climate, 17, 2413–2426, 2004. 26417
Joseph, P., Liebmann, B., and Hendon, H.: Interannual variability of the Australian summer monsoon onset – possible influence of Indian-summer monsoon and El-Nino, J. Climate, 4, 529–538, 1991. 26417
Kalnay, E., Kanamitsu, M., Kistler, R., Collins, W., Deaven, D., Gandin, L., Iredell, M., Saha, S., White, G., Woollen, J., Zhu, Y., Chelliah, M., Ebisuzaki, W., Higgins, W., Janowiak, J., Mo, K. C., Ropelewski, C., Wang, J., Leetmaa, A., Reynolds, R., Jenne, R., and Joseph, D.: The NCEP/NCAR 40-year reanalysis project, B. Am. Meteor. Soc., 77, 437–471, 1996. 26419
Kripalani, R. and Kulkarni, A.: Climatology and variability of historical Soviet snow depth data: some new perspectives in snow – Indian monsoon teleconnections, Clim. Dynam., 15, 475–489, 1999. 26417
Krishnamurthy, V. and Shukla, J.: Intraseasonal and interannual variability of rainfall over India, J. Climate, 13, 4366–4377, 2000. 26416
Krishnamurti, T., Han, S., and Misra, V.: Prediction of the dry and wet spell of the Australian monsoon, Int. J. Climatol., 15, 753–771, 1995. 26417
Kuhnel, I.: Tropical-extratropical cloudband climatology based on satellite data, Int. J. Climatol., 9, 441–463, 1988. 26427
Lawrence, D. and Webster, P.: Interannual variations of the intraseasonal oscillation in the south Asian summer monsoon region, J. Climate, 14, 2910–2922, 2001. 26416
Liu, X. and Yanai, M.: Influence of Eurasian spring snow cover on Asian summer rainfall, Int. J. Climatol., 22, 1075–1089, 2002. 26417
Livezey, R. and Chen, W.: Statistical field significance and its determination by Monte Carlo techniques, Mon. Weather Rev., 111, 46–59, 1983. 26431
Matsumoto, J.: The seasonal-changes in Asian and Australian monsoon regions, J. Meteor. Soc. Japan, 70, 257–273, 1992. 26417
Meehl, G.: The annual cycle and interannual variability in the tropical Pacific and Indian-ocean regions, Mon. Weather Rev., 115, 27–50, 1987. 26417
Meehl, G.: The south Asian monsoon and the tropospheric biennial oscillation, J. Climate, 10, 1921–1943, 1997. 26417
Meyers, G., McIntosh, P., Pigot, L., and Pook, M.: The years of El Nino, La Nina, and interac-

ACPD
11, 26415–26440, 2011

Australia-India teleconnection

S.-Y. Lee and T.-Y. Koh

tions with the tropical Indian ocean, J. Climate, 20, 2872–2880, 2007. 26425, 26427
Nicholls, N.: Sea surface temperatures and Australian winter rainfall, J. Climate, 2, 965–973, 1989. 26427
Nicholls, N.: All-India summer monsoon rainfall and sea-surface temperatures around Northern Australia and Indonesia, J. Climate, 8, 1463–1467, 1995. 26417, 26427
Onogi, K., Tslttsui, J., Koide, H., Sakamoto, M., Kobayashi, S., Hatsushika, H., Matsumoto, T., Yamazaki, N., Kaalhori, H., Takahashi, K., Kadokura, S., Wada, K., Kato, K., Oyama, R., Ose, T., Mannoji, N., and Taira, R.: The JRA-25 reanalysis, J. Meteor. Soc. Japan, 85, 369–432, 2007. 26423
Peixoto, J. P. and Oort, A. H.: Physics of Climate, Springer-Verlag, 1992. 26418
Perrin, G. and Simmonds, I.: The origin and characteristics of cold-air outbreaks over Melbourne, Aust. Meteo. Mag., 44, 41–59, 1995. 26426
Rajeevan, M., Pai, D. S., Kumar, R. A., and Lal, B.: New statistical models for long-range forecasting of southwest monsoon rainfall over India, Clim. Dynam., 28, 813–828, 2007. 26429
Rasmusson, E. and Carpenter, T.: The relationship between eastern equatorial Pacific sea-surface temperatures and rainfall over India and Sri-Lanka, Mon. Weather Rev., 111, 517–528, 1983. 26416
Saji, N., Goswami, B., Vinayachandran, P., and Yamagata, T.: A dipole mode in the tropical Indian Ocean, Nature, 401, 360–363, 1999. 26416
Simmonds, I. and Richter, T.: Synoptic comparison of cold events in winter and summer in Melbourne and Perth, Theor. Appl. Climatol., 67, 19–32, 2000. 26426
Singh, S., Kripalani, R., and Sikka, D.: Interannual variability of the Madden-Julian oscillations in Indian-summer monsoon rainfall, J. Climate, 5, 973–978, 1992. 26416
Sperber, K., Slingo, J., and Annamalai, H.: Predictability and the relationship between subseasonal and interannual variability during the Asian summer monsoon, Quart. J. Roy. Meteor. Soc., 126, 2545–2574, 2000. 26416
Tapp, R. and Barrell, S.: The North-west Australian cloud band, J. Climatol., 4, 411–424, 1984. 26427
Wilks, D.: Statistical methods in atmospheric sciences, Academic Press: San Diego, 1995. 26425, 26429, 26431
Yu, L., Jin, X., and Weller, R.: Annual, seasonal, and interannual variability of air-sea heat fluxes in the Indian Ocean, J. Climate, 20, 3190–3209, 2007. 26422

ACPD
11, 26415–26440, 2011

Australia-India teleconnection

S.-Y. Lee and T.-Y. Koh

Table 1. Correlations between gauge rainfall and VCD.

Name of station	Location (° E, ° N)	Correlation
Goa/Panjim	73.8, 15.5	0.82
Kozhikode	75.8, 11.3	0.77
Hissar	75.7, 29.2	0.75
Kota Aerodrome	75.9, 25.2	0.72
Kakinada	82.2, 17.0	0.69
Cuddalore	79.8, 11.8	0.65
Bikaner	73.3, 28.0	0.57
Jaipur/Sanganer	75.8, 26.8	0.54

ACPD
11, 26415–26440, 2011

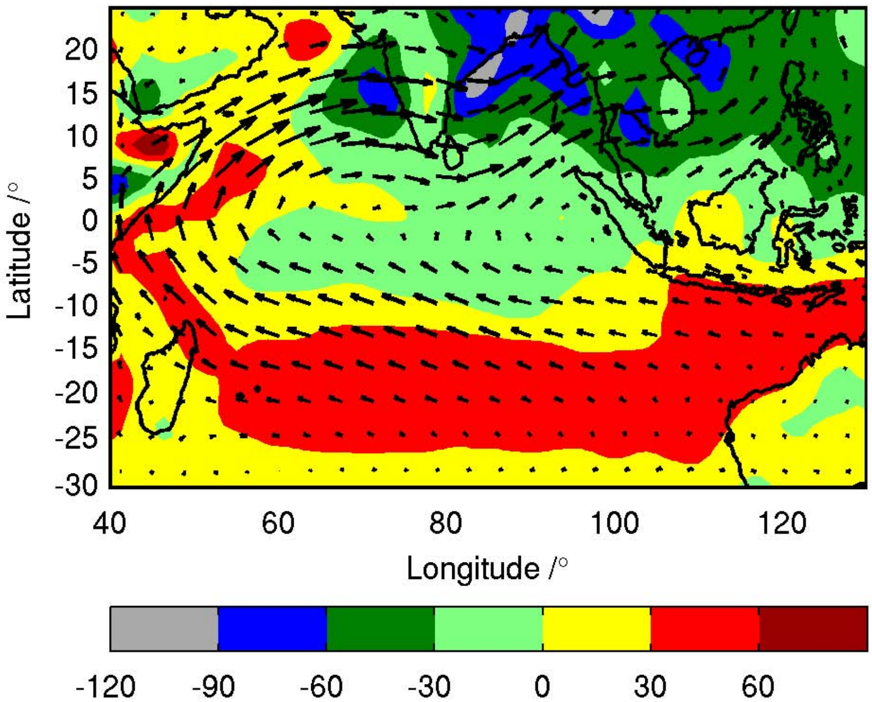

Fig. 1. Shading shows the net climatological source of water vapour in an air column (cm yr^{-1}), calculated using the convergence of vertically integrated water vapour flux (arrows) and water vapour time-tendency (not shown), from pentad averaged the Japanese 25-yr Reanalysis.

ACPD
11, 26415–26440, 2011

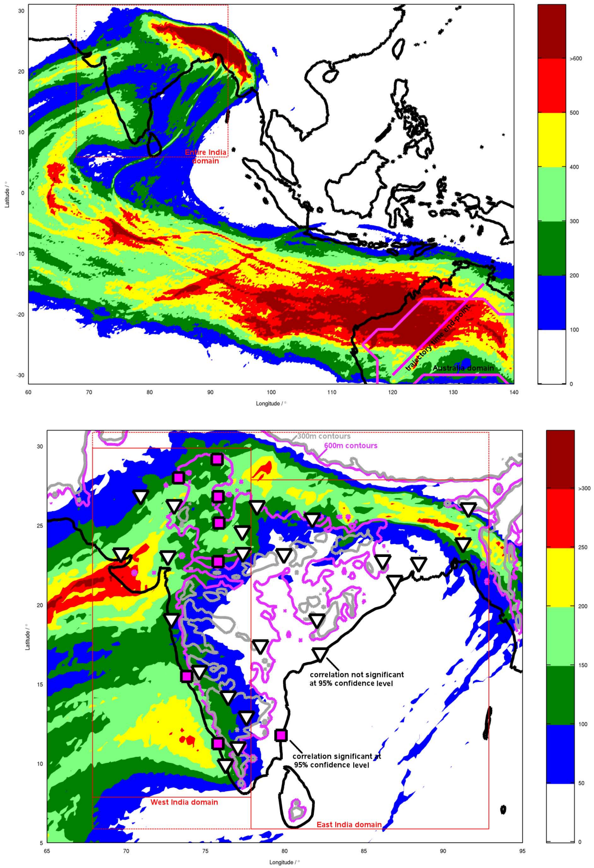

Fig. 2. Shading shows the number density of air parcel back-trajectories from India to Australia: **(a)** from the land regions of the Entire India domain; **(b)** from the land regions of the West India domain. Correlation between VCD and seasonal mean rainfall is calculated for rain gauges marked by squares and triangles in panel **(b)**.

ACPD
11, 26415–26440, 2011

Australia-India teleconnection

S.-Y. Lee and T.-Y. Koh

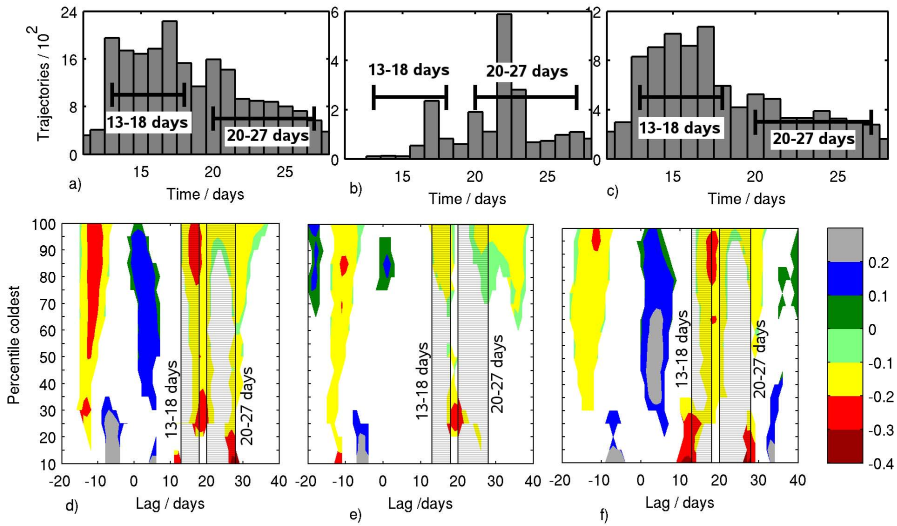

Fig. 3. (a) Histogram of back-trajectory times from the Entire India domain to Australia. **(b)** and **(c)** Same as **(a)** but for the East India and West India domains respectively. **(d)** Lag correlation, significant at 95 % confidence level, between Indian rainfall from TRMM and Australian temperature from NNRP for the Entire India domain. **(e)** and **(f)** Same as **(d)** but for the East India and West India domains respectively.

ACPD
11, 26415–26440, 2011

Australia-India teleconnection

S.-Y. Lee and T.-Y. Koh

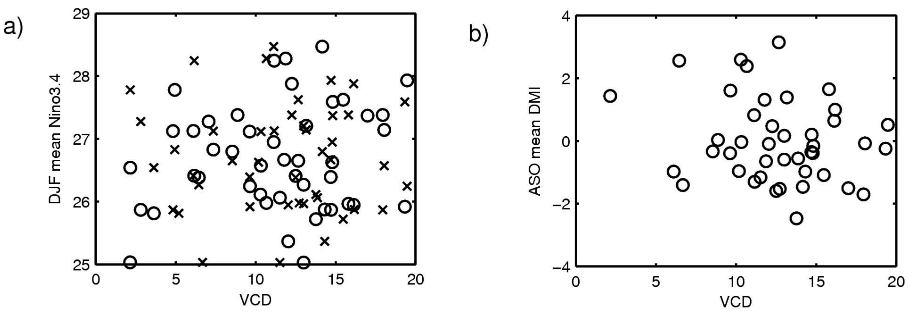

Fig. 4. Scatter plots of: **(a)** mean Nino3.4 in December-January-February (DJF) versus number of very cold days (VCD) in the same year (crosses) and the next year (circles) by the December month; **(b)** mean DMI in August-September-October versus VCD in the same year.

Discussion Paper | Discussion Paper | Discussion Paper | Discussion Paper |

ACPD
11, 26415–26440, 2011

Australia-India teleconnection

S.-Y. Lee and T.-Y. Koh

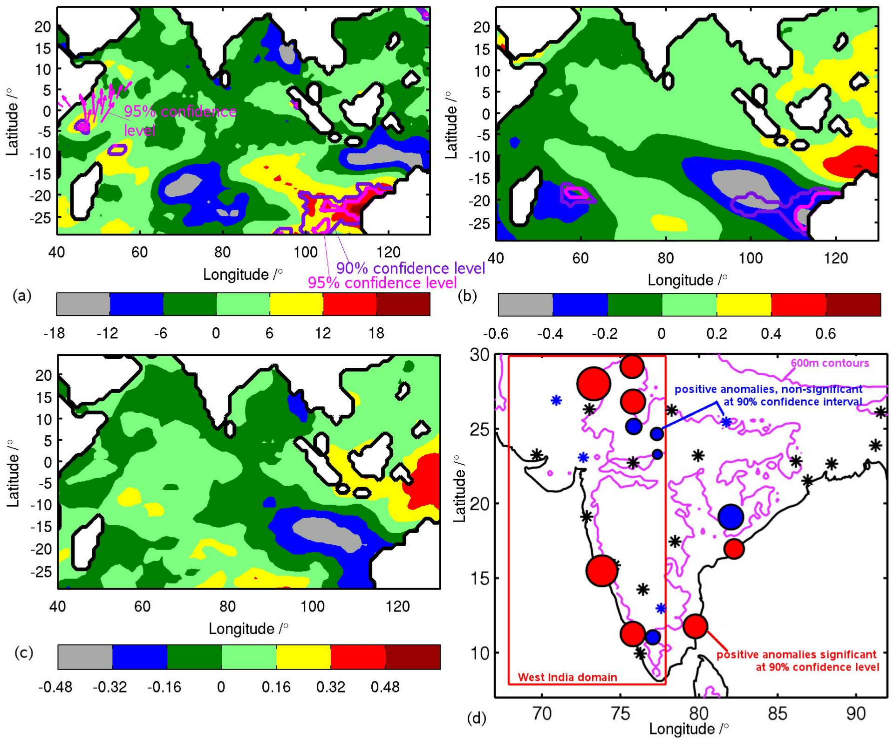

Fig. 5. (a) Composite for 1978, 1981, 1983, 1986, 1990 of anomalies of sea surface evaporation rate (cm yr^{-1}, shaded), 10 m-wind anomalies (arrows). **(b)** Same but for specific humidity at 2 m height (g kg^{-1}). **(c)** Same but for SST (K). **(d)** Mean anomalies of seasonal mean daily rainfall, normalized to the climatological standard deviation, *s*, of each rain gauge. Radius of circles are proportional to the mean anomalies (0.5 - 1.0*s*). Where the circle becomes too small to be clearly visible (< 0.15 s), it is replaced with an blue asterisk. Black asterisks mark stations that do not have a positive anomaly.

ACPD
11, 26415–26440, 2011

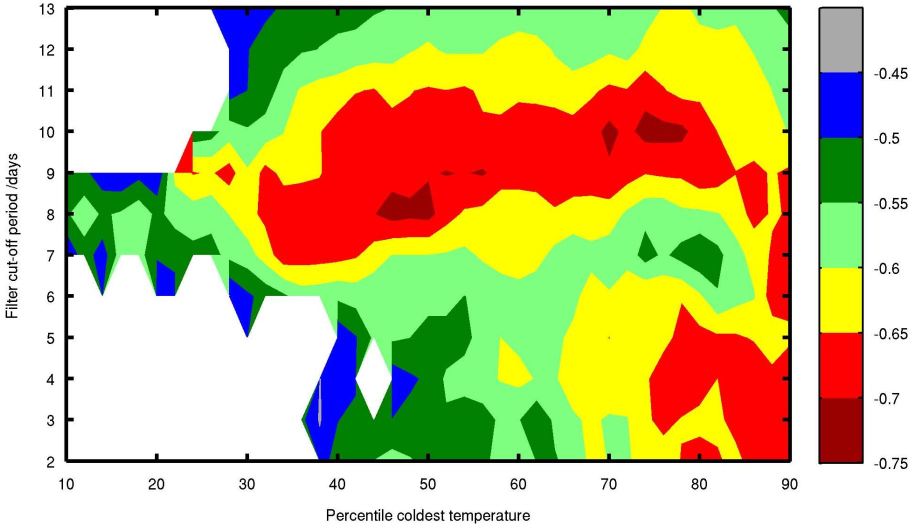

Fig. A1. Correlation coefficients between VCD and mean of temperatures below different percentile coldest temperatures after an *n*-day-to-2-month bandpass filter. Shaded regions are significant at 90 % confidence level.

ACPD
11, 26415–26440, 2011

Australia-India teleconnection

S.-Y. Lee and T.-Y. Koh